# Nature of nonradiative excitation-energy relaxation in condensed media with high activator concentrations

Yu. K. Voron'ko, T. G. Mamedov, V. V. Osiko, A. M. Prokhorov, V. P. Sakun, and I. A. Shcherbakov

*P. N. Lebedev Physics Institute, USSR Academy of Sciences*

Ion-ion interactions in the $LaF_3$-$NdF_3$ system are investigated in a wide range of variation of the $Nd^{3+}$ concentration, up to complete substitution of the $La^{3+}$ ions for the $Nd^{3+}$ ions. The decay kinetics of the metastable $Nd^{3+}$ $^4F_{3/2}$ state is determined for various temperatures and concentrations. The regions in which the decay is statically ordered, statically disordered, governed by migration, and occurs under conditions of ultrarapid energy migration (supermigration) are identified. The relationship between macro- and microparameters of the ion–ion interactions is found and their temperature dependences are determined. The temperature dependence of the interaction microparameter that leads directly to loss of electron excitation is determined by two independent methods. It is shown that energy migration over the $Nd^{3+}$ ions can in principle not be described in the framework of the generally accepted diffusion approach, and that loss of electron excitation as a result of their migration to the energy acceptors is a random Markov process. The conditions under which supermigration can occur are determined and it is shown that the metastable $Nd^{3+}$ $^4F_{3/2}$ state decays via energy supermigration at $NdF_3$ concentrations exceeding 10%. The microparameters of cross relaxation via a single intermediate level $^4I_{15/2}$ and of cross relaxation with participation of two intermediate levels $^4I_{13/2}$ and $^4I_{15/2}$ are determined. Quantitative agreement between the experimental and theoretical results is obtained.

PACS numbers: 71.70.Ms

## INTRODUCTION

The investigation of the fundamental problem of multipole interaction of impurity particles in condensed media has recently acquired special practical significance in view of the need for developing miniature lasers for integrated optics and optical-communication systems.

The principal requirement imposed on active elements of such lasers is high concentration of active ions, which brings about an effective interaction between them, and as a consequence a degradation of the energy of the electronic excitation into thermal vibrations. The presence of appropriate intermediate levels between the ground and excited states ensures effective cross relaxation, thereby increasing greatly the probability of nonradiative loss of excitation. This is precisely the shortcoming of the level scheme of $Nd^{3+}$, which is the most widely used activator of solid-state lasers, so that its concentration in the active element usually can not exceed 1–2 at.%. Recently, however, as a result of a search for new laser materials, reports have been published on lanthanum pentaphosphate crystals, in which the nonradiative losses from the metastable level of $Nd^{3+}$ are not very large even at 100% replacement of $La^{3+}$ with $Nd^{3+}$,[1,2] thus indicating that in principle the $Nd^{3+}$ can be used in highly concentrated systems. The way to solve this problem is to make a detailed investigation of the mechanisms that lead to the degradation of the excitation energy. The object of such investigations must satisfy the following basic requirements:

1. The crystals must be able to accept appreciable (desirably 100%) concentrations of the activator without a change in structure, must retain at the same time good optical quality, and must have sufficiently large dimensions.

2. The luminescence quantum yield at high concentrations should not be too low to make it difficult in principle to register the luminescence.

An analysis of the published data has shown that these conditions are satisfied by the system $LaF_3$–$NdF_3$. The technology of these crystals makes it possible to obtain large high-grade samples, with $LaF_3$ and $NdF_3$ forming a continuous series of solid solutions. To be sure, the luminescence quantum yield from the metastable state of $Nd^{3+}$ in the $NdF_3$ crystal is only $\sim 10^{-2}$–$10^{-3}$,[3] but at the present state of the physical experimental art it is possible to register reliably its radiation in a large dynamic range.

Until recently only the macroscopic parameters of the interaction could be determined in experiment as a rule, so that no unambiguous conclusions could be drawn concerning the processes that occur at the microscopic level. Consequently the experimental results obtained by different authors, even on the same objects, led frequently to directly contradictory conclusions.[3,4] Progress in theoretical research has made it possible to obtain the connection between the microscopic parameters of the interaction and the decay kinetics of the donor excitations, including also the case when the loss of the electronic excitation occurs under conditions when the energy migrates over the donor subsystems.[5-8] The results of the theory are illustrated in Fig. 1, where $t$ is the time and $\Pi(t)$ is a function that determines the kinetics of the nonradiative losses. The initial exponential section at $t<t_1$ is determined by the interaction with the energy acceptor at the minimum possible distance, say equal to the lattice constant. The slope $\frac{1}{2}$ in the time interval $t_1<t<t_2$, and consequently the nonradiative decay in the form

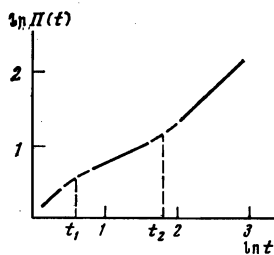$$e^{-\Pi(t)}, \quad \Pi(t)=\gamma\sqrt{t}, \tag{1}$$

FIG. 1. Kinetics of nonradia-
tive losses of donor excita-
tions $(e^{-\Pi(t)})$.

is determined by the direct donor-acceptor interaction
(Förster decay). The physical cause of its appearance
is the difference between the energy-transfer probabili-
ties from the different donors in the dipole–dipole in-
teraction, due to the different configurations of their
acceptor environment. Since expression (1) has a de-
rivative that diverges at the point $t = 0$, meaning physi-
cally an infinite rate of loss of excitation at the initial
instant of time, the presence of a short exponential sec-
tion on the initial section of the decay is of principal
significance. It was observed experimentally in[9].

The exponential decay during the final stages of the
process $(t > t_2)$ is determined by the migration of the ex-
citation over the donors to the acceptor, where it is
annihilated. In real systems one should frequently ex-
pect the parameter of the interaction that causes the en-
ergy migration $(C_{DD})$ to be larger than the parameter of
the interaction that leads directly to the loss of the ex-
citation $(C_{DA})$:

$$C_{DD} > C_{DA} \qquad (2)$$

or even

$$C_{DD} \gg C_{DA}, \qquad (2a)$$

$$W_{DD}(R) = C_{DD}/R^s, \qquad W_{DA}(R) = C_{DA}/R^s. \qquad (3)$$

Here $W_{DD}(R)$ is the migration probability, or the num-
ber of jumps of the excitation over the metastable state
per unit time at a distance $R$ between the interacting
particles. $W_{DA}(R)$ is the probability of the loss of the
excitation, or the number of nonradiative acts of loss of
excitation per unit time at a distance $R$ between the in-
teracting particles; $s = 6$, 8, or 10, depending on the
multipolarity of the interaction. The parameters $C_{DD}$
and $C_{AA}$ are determined by the oscillator strengths and
by the overlap integral of the interacting transitions.

The annihilation of the electronic excitation via migra-
tion to the acceptor, under conditions (2) and (2a), can
not be described in principle within the framework of
the customary diffusion approach, which is valid only
in the case $C_{DA} \gg C_{DD}$.[6–10] This condition means phys-
ically that a density gradient of the donor excitations
exists in a certain region around the acceptor. An im-
portant factor of the theory was therefore the develop-
ment of the hopping mechanism of the migration[6–8] as
an alternative of the diffusion approach. In contrast to
the diffusion approximation, the hopping mechanism is
the consequence of considering the annihilation of the
excitation by migration, when the migration-induced
fluctuations of the rate of the nonradiative decay can be
described by a Markov process without correlation.

The region of its applicability is given by conditions (2)
and (2a). The connection between the experimentally
measured values and the microscopic parameters of the
interaction, the temperature and concentration depen-
dences of which are determined by the interaction mech-
anisms and contain information concerning the latter,
turns out to be quite different in these two cases. In
addition, the different theories give identical results
only in the limiting cases

$$\Pi(t) = \begin{cases} \gamma(t)^{\nu_2}, & t \ll t_2 \\ Wt, & t \gg t_2 \end{cases}. \qquad (4)$$

There is no meeting of the minds concerning the situa-
tion in the transition regions, concerning the dimen-
sions of these regions, and concerning the connections
between the limiting times $t_1$ and $t_2$ at different activator
concentrations. This provides a leeway in the reduction
of the experimental results. We have advanced in[11,12]
certain ideas on this subject. The presently available
experimental data, however, are patently insufficient
to be able to draw final conclusions. Such data can be
obtained only by investigating the kinetics of the decay
of the donor excitations in a large dynamic range and in
a wide region of concentrations and temperatures.

## INVESTIGATED CRYSTALS AND EXPERIMENTAL PROCEDURE

The $LaF_3$–$NdF_3$ crystals were grown from the melt
by the dropping-crucible method, using a fluoriding
atmosphere and the procedure of[13]. The concentration
$C$ of the $NdF_3$ was 0.3, 1, 2, 3, 5, 10, 30, 50, 90, or
100 at.%. Spectral-luminescence investigations were
carried out by the procedures described in[9,11,14].
Smooth variation of temperature from 4.2 to 300 °K and
maintenance of constant sample temperature were en-
sured by the use of the cryogenic system of the UTREKS
type or using a CF-204 cryostat made by the Oxford In-
struments Company.

The decay curves of the excited state of $Nd^{3+}$ were ob-
tained by the procedure of[11]. The luminescence was
excited by a periodic-pulsed rhodamine-6G tunable
laser, described in[15], with pulse duration 15 nsec.

## EXPERIMENTAL RESULTS

To obtain information on the nonradiative decay it is
necessary to know the probability of the radiative tran-
sitions from the metastable state. When working at low
concentrations, this problem is trivial. At low $Nd^{3+}$
concentrations, when the measured lifetime $\tau_{meas}$ does
not depend on the concentration, the measured quantity
is the radiative lifetime $\tau_0$, since the probability of
multiphonon internal relaxation from the metastable
state $^4F_{3/2}$ of the $Nd^{3+}$ ions in the crystals is small.[16,17]
At appreciable activator concentrations, the parameters
of the crystal field, both even and odd, can change, and
this leads to a change in the radiative probabilities and
to a change in the energies of the Stark components of
the interacting transitions. An analysis of the optical
spectra of the investigated crystals has made it possible
to construct the level schemes of the crystal splitting of
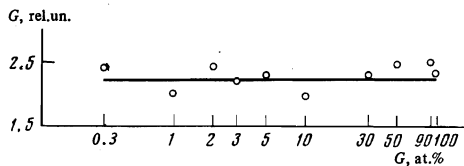the ground and excited terms and to observe certain

FIG. 2. Dependence of the relative absorption on the $NdF_3$ concentration in an $LaF_3$ crystal.

changes in these schemes as functions of the $NdF_3$ concentration. It turned out that when the $NdF_3$ concentration changes from 2 to 100 at.%, the energies of the Stark components of the levels $^4F_{3/2}$ and $^4I_{15/2}$ change somewhat, and this can influence the effectiveness of the cross-relaxation process. Thus, the energy of the lower component of the $^4F_{3/2}$ was increased by 2 cm$^{-1}$, and the energy of the lower component of the $^4I_{15/2}$ level was decreased by 9 cm$^{-1}$, leading to a decrease, from 32 to 12 cm$^{-1}$, in the anti-Stokes mismatch in the interaction of the transitions $^4F_{3/2} \rightarrow {}^4I_{15/2}$ and $^4I_{9/2} \rightarrow {}^4I_{15/2}$ at $T = 4.2$ °K.

In the entire investigated range of concentrations, we have verified also satisfaction of the Bouguer–Lambert–Beer law. Its satisfaction offers evidence that the values of the Einstein coefficients remain unchanged when the activator content is changed. Since the range of variation of the $NdF_3$ concentration was very large, it was impossible to attain the optical densities needed to measure the integral absorption coefficients in the chosen characteristic groups by merely varying the thicknesses of the investigated samples. To obtain the plot of Fig. 2 we used practically all the transitions contained in the transparency region of the $LaF_3$ lattice. When the $NdF_3$ concentration was changed, the optical spectra did not reveal any redistribution of the intensi-

ties of the transitions coupling the individual Stark components of the ground and excited states, thus indicating that the investigated samples had the same crystallographic orientation. At concentrations 5, 30, and 50 at.% $NdF_3$ we effected the corresponding renormalizations and changed over to a measurement of the integral absorption in bands having different intensities. It turns out that the Bouguer–Lambert–Beer law is satisfied in the entire range of the investigated concentrations (Fig. 2), i.e., the radiative lifetime remains unchanged at all concentrations.

The results of the kinetic measurements are shown in Fig. 3. A strictly exponential decay was observed not in all cases by far, although an exponential behavior was always reached during the final stages of the process. The large dynamic range of the measurements has made it possible to verify this with a great degree of accuracy. If the decay was not exponential during the initial range of the observation time, then the values of $\tau_{meas}$ shown in Fig. 3 correspond to subsequent exponential stages of the process. At a concentration 0.3 at.% $NdF_3$, the temperature dependence of $\tau_{meas}$ is weak ($\tau_{meas} = 750$ μsec at 4.2 °K and 680 μsec at 300 °K). This dependence is due only to the difference between the combined probabilities of the radiative transitions from the ground and excited components of the excited state $^4F_{3/2}$.[14] At $C = 2$ at.%, the equality $\tau_{meas} = \tau_0 = 750$ μsec holds only at temperatures 4.2–10 °K, and $\tau_{meas}$ decreases with further increase of temperature. The plateau in the temperature region 4.2–10 °K is observed at all concentrations, but the absolute values of $\tau_{meas}$ become less than the radiative value as the concentration is increased. In the crystals investigated by us, deviation from exponential decay was observed at $C = 2$ at.% in the temperature region 30–300 °K, at $C = 3$ at.% in the region 70–300 °K, and at 5 at.% in the region 150–300 °K. At $C = 10$ at.%, a slight deviation from exponential is observed only at room temperature. In all the remaining cases, the decay is strictly exponential. Examples of the decay curves ($I_{lum} = f(t)$) are shown in Fig. 4. Figure 5 shows the temperature dependences of the probability of nonradiative deactivation ($W_{deact}$) of the metastable state:
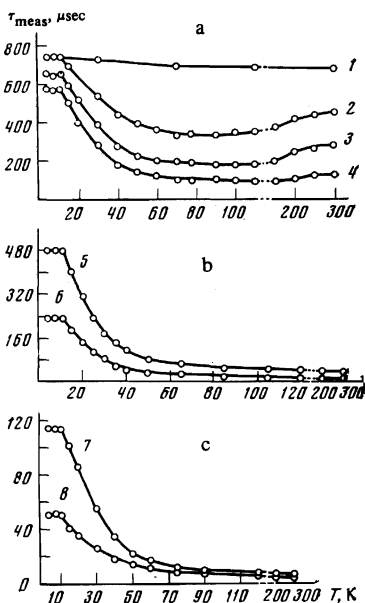
$$W_{deact} = -1/\tau_{meas} - 1/\tau_0 . \qquad (5)$$

The values of $\tau_0$ include the temperature correction re-



FIG. 3. Temperature dependence of $\tau_{meas}$ at different $NdF_3$ concentrations ($C$, at.%) in the $LaF_3$ crystal: a) 1—$C = 0.3$, 2—$C = 2.0$, 3—$C = 3.0$, 4—$C = 5.0$; b) 5—$C = 10$, 6—$C = 30$; c) 7—$C = 50$, 8—$C = 90$; 100.
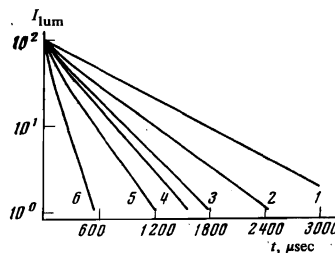


FIG. 4. Decay of excited $^4F_{3/2}$ metastable state of $Nd^{3+}$ in $LaF_3$ crystals at various $NdF_3$ concentrations and at the following temperatures: 1—$C = 2$, $T = 4.2$; 2—$C = 2$, $T = 30$; 3—$C = 2$, $T = 46$; 4—$C = 2$, $T = 77$; 5—$C = 3$, $T = 300$; 6—$C = 5$, $T = 240$.
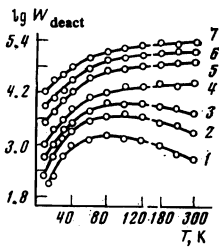
FIG. 5. Temperature dependence of the probability of nonradiative deactivation of excited $^4F_{3/2}$ metastable state of $Nd^{3+}$ in $LaF_3$ crystal at the following $NdF_3$ concentrations: 2 at.% (1), 3 at.% (2), 5 at.% (3), 10 at.% (4), 30 at.% (5), 50 at.% (6), 100 at.% (7).

ferred to above. The temperature dependences of $W_{deact}$ for 90 and 100 at.% $NdF_3$ are practically the same.

## ANALYSIS AND DISCUSSION OF RESULTS

It is seen from Fig. 5 that the $\log W_{deact} = f(T)$ curves break up into two families, depending on the $NdF_3$ concentration. At concentrations 2–5 at.% a maximum is observed in the temperature region $\sim 80$ °K, whereas at concentrations higher than 10 at.% there is no such maximum and the weak growth of $W_{deact}$ continues up to room temperatures. In the low-temperature region, the plots at low concentrations are even steeper. Consequently, the temperature affects differently the deactivation of the metastable state at different activator concentrations. One more difference is observed in the kinetics of the decay of these two groups of crystals. The deviation from the exponential law during the initial stages of the process takes place only at $NdF_3$ concentrations from 2 to 10 at.%. It has also turned out that at $NdF_3$ concentrations up to 5 at.% the value of $W_{deact}$ is proportional to the square of the total activator concentration ($W_{deact} \propto C^2$) (Fig. 6a), whereas at large concentrations we have $W_{deact} \propto C$ (Fig. 6b).

The treatment of the migration with subsequent annihilation of the excitation in the interaction with the acceptor as a Markov process (the hopping model) yields the following expression for the constant of the nonradiative decay due to the energy migration in dipole–dipole interactions[6,7]:

$$\bar{W} = \pi (2\pi/3)^{1/2} n_A n_D (C_{DA} C_{DD})^{1/2}, \qquad (6)$$

where $n_A$ and $n_D$ are the numbers of acceptors and donors in 1 cm³. The probability (6) is determined by the migration of the excitations, which annihilate when they fall into the sphere of the strong $D$–$A$ interaction. The radius $R_W$ of this sphere is introduced on the basis of the condition

$$C_{DA} \tau_W / R_W^6 = 1, \qquad (7)$$

where $\tau_W$ is the time of passage of the excitation through the region enclosed in this sphere. As already indicated, the types of decay in the diffusion and hopping theories are the same. The asymptotic forms in (4) coincide as $t \to 0$ and $t \to \infty$. The difference between these models manifests itself when it comes to calculate the

connection of $\bar{W}$ with $C_{DA}$ or $C_{DD}$. The hopping theory, and consequently expression (6), is valid under conditions (2) and (2a). The diffusion theory is valid in the opposite case $(C_{DA} \gg C_{DD})$. In the latter case, taking into account the irregular arrangement of the donor particles (quasi-diffusion), the following connection was proposed in[6] between $\bar{W}$ and $C_{DA}$ and $C_{DD}$:

$$\bar{W} = \frac{(4\pi)^2}{3} \left( \frac{1}{2} \right)^{1/4} n_A n_D C_{DA}^{1/4} C_{DD}^{3/4}. \qquad (8)$$

Expression (8) was derived in[6] on the basis of the result of[5]

$$W = 0.676 \cdot 4\pi n_A C_{DA}^{1/4} D^{3/4},$$

where $D$ is the diffusion coefficient, except that $D$ was replaced by a quasi-diffusion coefficient introduced in a definite manner. In[8] there were also obtained expressions for $\bar{W}$ for the case $C_{DD} \gg C_{DA}$:

$$\bar{W} = \frac{2\pi^2 c_A c_D}{\Omega^2} (C_{DA} C_{DD})^{1/2}, \qquad (9)$$

as well as for the case $C_{DA} \gg C_{DD}$ with allowance for the irregular arrangement of the donors and acceptors:

$$\bar{W} = \frac{2.85\pi^2 c_A c_D}{\Omega^2} C_{DA}^{1/4} C_{DD}^{3/4}. \qquad (10)$$

Here $\Omega$ is the volume per donor or acceptor, $c_D$ and $c_A$ are the relative concentrations of the donors and acceptors ($c_D = 1$ corresponds to the regular sublattice of donor ions). It must be noted that formulas (8) and (10), which describe the quasi-diffusion case, differ significantly. On the other hand, the expressions (6) and (9) for the hopping mechanism, which were obtained by entirely different methods, agree apart from the numerical coefficients.

It is seen from (6) and (8)–(10) that in all the models the concentration dependence of $\bar{W}$ is the same. Thus, on the basis of the experimental result $W_{deact} \sim n^2$ (where $n$ is the number of $Nd^{3+}$ ions in 1 cm³) in the concentration region up to 5 at.% $NdF_3$, we can conclude that $n_A = n_D = n$ and the annihilation of the electronic excitation is due directly to the cross relaxation, while the expo-
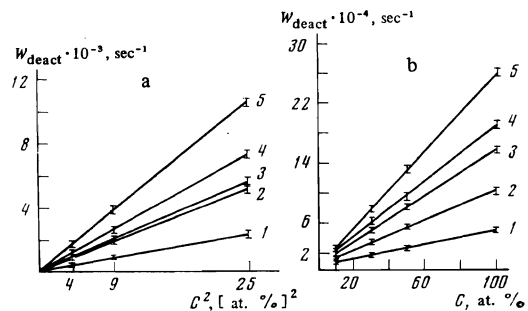


FIG. 6. Concentration dependence of the probability of nonradiative deactivation of the excited metastable $^4F_{3/2}$ state of $Nd^{3+}$ in the $LaF_3$ crystal at different temperatures (in °K): a) 1—30; 2—40; 3—300; 4—180; 5—120; b) 1—40; 2—60; 3—77; 4—120; 5—300.

nential kinetics at the final stages of the process, with a constant smaller than the radiative constant, is due in the indicated concentration region to the energy migration over the $Nd^{3+}$ ions. However, to draw any conclusions concerning the migration mechanism and to extract information on its microscopic cause, it is necessary to have information on the ratio of the quantities $C_{DA}$ and $C_{DD}$. The experimentally observed linearization of the concentration dependence of $W_{deact}$ at high $NdF_3$ concentrations can be interpreted from two points of view, which become identical in the limiting case of a regular $NdF_3$ lattice. Namely, the rate of nonradiative annihilation of the excitation, which is linear in the $Nd^{3+}$ concentration, can occur either at the initial stage of the decay process[8] or as a result of an ultrafast excitation migration.[1)] The initial exponential section of the decay, as already noted, is due to the fact that in the crystal the distance between the donor and the acceptor cannot be smaller than the maximum possible distance between the sites of the sublattice made up of the sites accessible to the $Nd^{3+}$ ion (in our case this is the La sublattice). In this section, the decay proceeds at a rate[8]

$$c \sum_R W_{DA}(R). \tag{11}$$

The summation in (11) is over the sites of the lanthanum sublattice. After a time $t_1$ (see Fig. 1) the exponential decay (11) gives way to a decay of the type (1). At not too large concentrations, the value of $t_1$ can be estimated from[8]

$$t_1 \gtrsim \Omega^2 / C_{DA}. \tag{12}$$

In this case $\Omega = V/N_{La} = c/n$ is the volume per $La^{3+}$ ion ($V$ is the sample volume and $N_{La}$ is the total number of $La^{3+}$ ions). Expression (12), as well as all the relations that follow, holds if the elementary acts of the migration and quenching excitation transfer have a dipole–dipole character.

It is easy to establish a criterion for the realization of the supermigration mechanism of excitation annihilation. In the region of not too high $Nd^{3+}$ concentrations, the supermigration sets in at concentrations such that the average rate of the migrational excitation transfer begins to exceed the largest possible rate of its annihilation:

$$C_{DD}/\bar{R}^6 > C_{DA}/\Omega^2, \tag{13}$$

where $\bar{R} \approx (\Omega/c)^{1/3}$ is the average distance between the $Nd^{3+}$ ions. When condition (13) is satisfied, the donor populations become equalized, after which it is necessary to put $p(R_i) = p(R_k) = p(i \neq k)$ in the fundamental kinetic equations

$$\frac{dp(R_i)}{dt} = -p(R_i) \sum_k W_{DD}(R_{ik}) + \sum_k W_{DD}(R_{ik}) p(R_k)$$
$$-p(R_i) \sum_l W_{DA}(R_{il}) - \frac{p(R_i)}{\tau_0} \tag{14}$$

($R_i$ are the sites occupied by the $Nd^{3+}$ ions, $p(R_i)$ is the

population of the donor in the site $i$, and $R_{ik}$ is the distance between the sites $i$ and $k$), and a result we obtain for the total donor population $N = \sum_i p(R_i)$

$$\frac{dN}{dt} = -p \sum_{i,l} W_{DA}(R_{i,l}) - \frac{N}{\tau_0} = -cN \sum_R W_{DA}(R) - \frac{N}{\tau_0}, \tag{15}$$

i.e., the nonradiative decay will follow the same exponential law as (11). Thus, the same type of decay (11), as already indicated, can be caused by different factors, thus raising the question of experimentally identifying the dependence observed by us with one of the mechanisms described above. This can be done by tracing the variation of the nonradiative-decay curves in a wide range of values of $c$.

We consider the limiting cases

$$C_{DD} \gg C_{DA}, \tag{16}$$

$$C_{DD} \ll C_{DA}. \tag{17}$$

We find from (13) that in a sample that is not too concentrated the ultrafast migration takes place at a concentration $c > c^*$, where

$$c^* \approx (C_{DA}/C_{DD})^{1/2}, \tag{18}$$

i.e., under condition (16) the singly-exponential decay with rate (11) will take place even at sufficiently low temperatures ($c^* \ll 1$). At $c < c^*$, the decay process breaks up into three stages (Fig. 7a): an initial exponential stage with exponent $tc \sum_R W_{DA}(R)$ (region I, $0 < t < t_1$) goes over into a Förster curve (region II, $t_1 < t < t_2$), which again goes over into an exponential (region III, $t > t_2$), but now due to the migration of the energy.[8] The "instant" $t_2$ of transition to the migrational exponential can be obtained by equating the arguments of the exponentials of the Förster decay (1):

$$\gamma = \frac{4}{3} \pi^{3/2} n_A \sqrt{C_{DA}} \tag{19}$$

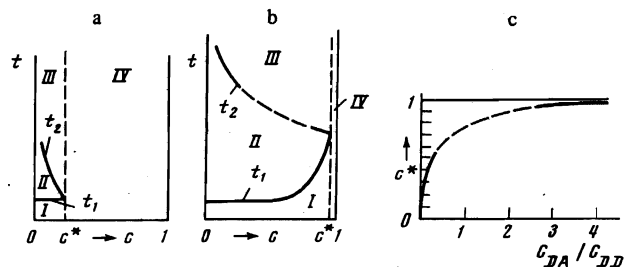and the migration decay (6) or (9). As a result we obtain



FIG. 7. Different sections of the nonradiative decay curve and the dependence of the critical concentration $c^*$ on the ratio $C_{DA}/C_{DD}$. Regions: I—statically ordered decay; II—statically disordered decay; III—migrational decay; IV—supermigration; $t_1$—limiting time of transition from static ordered decay to static disordered decay, $t_2$—limiting time of transition from static disordered decay to migration decay; $c^*$—critical concentration of the transition to the decay under conditions of energy supermigration; a—case $C_{DD} \gg C_{DA}$; b—case $C_{DD} \ll C_{DA}$; c—dependence of $c^*$ on the ratio of the microscopic parameters of the interaction.

$$t_2 = 4\Omega^2/9\pi c^2 C_{DD}. \tag{20}$$

Comparison of this expression with $t_1$ from (12) shows that at $c \approx c^*$ the time $t_1$ coincides approximately with $t_2$, i.e., the Förster kinetics does not appear at any time at all, while the initial exponential (11) goes over immediately into the supermigration exponential, this transition being continuous in the sense that at $c \approx c^*$ the rate of decays (6), (9), and (11) coincide and become the single rate of the supermigration decay. Thus, four sections can be distinguished on the $(t, c)$ plane, each characterized by its own mechanism of nonradiative annihilation of the excitation (Fig. 7a): region I—static "ordered" decay, II—static "disordered" decay, III—decay due to hopping migration of the energy, and IV—decay due to supermigration. Regions I and II, on the one hand, and II and III, on the other, are separated by diffuse boundaries determined from (12) and (20). At $c > c^*$, regions I, III, and IV turn out to be "joined together," i.e., the rates of all three decays (I, III, and IV) are identical.

In the other limiting case $(C_{DD} \ll C_{DA})$ the law governing the decay at arbitrary $Nd^{3+}$ concentrations is given in first-order approximation by

$$\exp \sum_n \ln[1 - c + c \exp\{-t W_{DA}(R)\}]. \tag{21}$$

It follows from (18) that no transition to supermigration at low and medium concentrations is possible at $C_{DD} \ll C_{DA}$. As $c \to 1$, however, decay with supermigration rates (11) can be realized, and the corresponding concentration can be determined in the following manner.

It is seen from (21) that as $c \to 1$ the limiting time $t_1$ has a logarithmic singularity

$$t_1 \sim \frac{\Omega^2}{C_{DA}} |\ln(1-c)|. \tag{22}$$

At the same time the quantity $\Gamma = t_1^{-1}$, obviously, characterizes the scatter of the individual decay rates for the different ions. If the migration rate $C_{DD}/\Omega^2$ exceeds $\Gamma$, then the populations of the donors become equalized, after which a decay of type (11) appears again. We note incidentally that the relation (13) means none other than that the migration rate exceeds the scatter of the decay rates, but at concentrations not close to unity. Indeed, the distribution function of the decay rates, as is well known, is given by

$$\varphi(W_{DA}) = \gamma \left( \frac{1}{4\pi W_{DA}^3} \right)^{1/2} \exp\left( -\frac{\gamma^2}{4 W_{DA}} \right).$$

In crystals this expression is valid at $c \ll 1$ and $W_{DA} < W_{max}$, where $W_{max}$ is the maximum possible decay rate, i.e., $\varphi(W_{DA}) = 0$ at $W_{DA} > W_{max}$. This circumstance changes somewhat the normalization of the function $\varphi(W_{DA})$, but this is immaterial here. A characteristic feature of the function $\varphi(W_{DA})$ is its slow decrease as $W_{DA} \to \infty$, so that we even have

$$\langle W_{DA} \rangle = \int_0^\infty dW_{DA} W_{DA} \varphi(W_{DA}) = \infty.$$

Therefore, if we recognize that at $c \ll 1$ the function $\varphi(W_{DA})$ reaches its maximum at the value $W_{DA}^* = \gamma^2/6 \ll W_{max}$, the role of the width $\Gamma$ of the decay-rate spectrum will be assumed by $W_{max}$, as is indeed fixed in (13). On the other hand, as $c \to 1$, the function $\varphi(W_{DA})$ is maximal near $W_{DA} \approx W_{max}$, and this explains the narrowness of the decay-rate spectrum in this case. Thus, as $c \to 1$ the condition for realizing a decay of the type (11) is

$$C_{DD} > C_{DA}/|\ln(1-c)|, \tag{23}$$

i.e.,

$$c^* = 1 - \exp(-C_{DA}/C_{DD}). \tag{24}$$

An approximate plot of $c^* = f(C_{DA}/C_{DD})$, constructed on the basis of (18) and (24) is shown in Fig. 7c. To establish the concentration dependence of the limiting time $t_2$ in the limit $C_{DD} \ll C_{DA}$, we use relation (10), which was obtained for this case, and formula (19). As a result we have

$$t_2 \sim \frac{\Omega^2}{16c^2} \frac{C_{DA}^{5/3}}{C_{DD}^{5/3}}. \tag{25}$$

An estimate of $t_2$ using instead of expression (10) the expression (8), which was also obtained in the quasi-diffusion model (i.e., it should describe the situation $C_{DA} \gg C_{DD}$), but differs from (10), alters $t_2$ only insignificantly. In formula (25) the exponents $\frac{2}{3}$ and $\frac{5}{3}$ are replaced by $\frac{1}{2}$ and $\frac{2}{3}$ respectively, and this does not affect the estimates that follow.

It is seen from Figs. 7a and 7b that in both cases $(C_{DD} \gg C_{DA}$ and $C_{DA} \gg C_{DD})$ it is possible, by increasing the concentration, to obtain ultimately a nonradiative-decay kinetics that is linear in $C$, even if a Förster-type decay is observed at low concentrations (i.e., region II, Figs. 7a and 7b). Figure 7 shows, however, that in the case when such a transformation takes place at $c^* \ll 1$, the condition $C_{DD} \gg C_{DA}$ is bound to be satisfied. The experimental value of $c^*$, as already noted, is $\lesssim 0.1$. Furthermore, the least favorable, from our point of view, estimate of $t_2$ in accordance with (25), at $c = 0.02$, yields $t_2 > 10^{-3} - 10^{-2}$ sec, whereas experiment gives $t_2 < 10^{-4}$ sec. The two facts indicate that in the $LaF_3 - NdF_3$ system we have the situation $C_{DD} \gg C_{DA}$ with all the consequences that ensue in accordance with Fig. 7, and that the decay of the excited state $^4F_{3/2}$ at $C > 10$ at.% $NdF_3$ takes place under supermigration conditions. It follows also that the energy migration over the $Nd^{3+}$ ions cannot be described within the framework of the diffusion theory, and that the excitation dissipation process in the case of interaction with the acceptors as a result of the energy transport over the metastable state is a random Markov process. Consequently, to determine the parameter $C_{DD}$ it is necessary to use expression (6) or (9) at $C < 10$ at.% $NdF_3$. We note that a decay at the rate (11) is possible also in the static case (i.e., in the absence of excitation migration over the donors), but only at very large acceptor concentrations. This formally brings closer together the statistic decay to

256     Sov. Phys. JETP, Vol. 44, No. 2, August 1976

Voron'ko et al.     256

the decay under conditions of ultrafast migration in the objects investigated by us, and makes them indistinguishable, in principle, in the regular $NdF_3$ lattice.

All the foregoing results in two independent methods of determining the microscopic interaction parameter $C_{DA}$. The first—kinetic—method is based on an analysis of the form of the decay in its exponential section. This method, generally speaking, is ambiguous for two reasons:

1) the use of the asymptotic formulas (4) provides a leeway in the analysis of the decay kinetics[6,9,11];

2) expression (19), which connects the experimentally determined parameter $\gamma$ with the microscopic interaction parameter $C_{DA}$, was obtained by calculation with a certain model, the equivalence of which to the real situation must be proved.

The second method, that of calculating the lattice sum, is "model-independent" and is based only on measurement of the constant of the exponential decay at high concentrations, on the knowledge of the structure of the $LaF_3$ crystal, and on the assumption that the probabilities are additive, [18] an assumption which is subject to no doubt in our case, inasmuch as in the objects investigated by us the rate of the phase relaxation greatly exceeds the deactivation. In other words, the observed level widths exceed by several orders of magnitude the decay rate even under conditions of a regular lattice of interacting ions.[19,20] We then obtain for the generalized probability[18]

$$Q = \sum_p Q_p = \sum \frac{\omega_p}{1+\omega_p\tau_a},$$ (26)

where $\omega_p$ is the probability due to the interaction with the $p$-th acceptor, $\tau_a$ is the lifetime of the acceptor level, and the summation is over the acceptor ions.

The mechanism of cross relaxation via the levels of the term $^4I$, as well as the structure of the ground-state term, which ensures on account of the electron-phonon interaction the satisfaction of the condition

$$\omega_p\tau_a \ll 1,$$

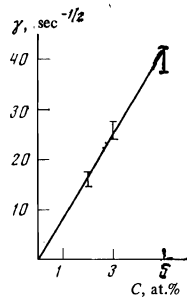excludes the possibility of reverse energy transfer, and thus

FIG. 8. Analysis of the function $\Pi(t)$, $\alpha = 2.3$. a) $T = 300\,°C$, $C = 3$ at.%, curves 1—the function $\alpha^{-1}\Pi(t)$, 2—the function $\alpha^{-1}\overline{W}t$, 3—the function $\alpha^{-1}[\Pi(t) - \overline{W}t]$. b) the function $\alpha^{-1}[\Pi(t) - \overline{W}t] = f(\sqrt{t})$: 1—$C = 3$ at.% $NdF_3$, $T = 300$ K; 2—$C = 3$ at.% $NdF_3$, $T = 90$ K; 3—$C = 2$ at.% $NdF_3$, $T = 77$ K; 4—$C$ at.% $NdF_3$, $T = 46$ K.

FIG. 9. Concentration dependence of $\gamma$ at $T = 300\,°K$.

$$W_{\text{deact}} = \sum \omega_p,$$ (27)

i.e., the applicability of (27) is rigorously demonstrated.

## Kinetic method of determining $C_{DA}$

As indicated above, the experimentally observed decay is not exponential at low $NdF_3$ concentrations. An analysis of the non-exponential kinetics will be carried out by the method proposed by us in[11]. We represent the observed decay curves in the form

$$N(t) = N_0 \exp[-(t/\tau_0 + \Pi(t))].$$ (28)

The obtained experimental data make it possible to determine the form of the function $\Pi(t)$ by subtracting, in a semi-logarithmic scale, the normalized curves of the observed decay from the radiative decay. An example of the experimentally obtained function $\Pi(t)$ is shown in Fig. 8a. We see that at sufficiently long times this function turns out to be proportional to the time. The slope is determined by the quantity $\overline{W}$. Further, subtracting $\overline{W}t$ from $\Pi(t)$ (Fig. 8a), we find that the difference curve $[\Pi(t) - \overline{W}t]$ varies with time like $\sqrt{t}$ (Fig. 8b). Thus, the function $\Pi(t)$ takes the form

$$\Pi(t) = \gamma\sqrt{t} + \overline{W}t.$$ (29)

The limiting time $t_2$ in this actual case turns out to be

$$t_2 = (\gamma/\overline{W})^2 = 2 \cdot 10^{-4} \text{ sec}.$$

By analyzing in this manner all the non-exponential decay curves at different temperatures and concentrations, we have obtained the dependence of $\gamma$ on the concentration (Fig. 9) and on the temperature (Fig. 10). It is seen from Fig. 9 that $\gamma$ depends linearly on the concentration. At $t < t_2$, the condition $\gamma\sqrt{t} \gg \overline{W}t$ is not satisfied in the entire investigated time interval of the decay, i.e., the condition under which the "Förster" asymptotic form (4) is reached is not realized in the experiment. However, in all the non-exponential-decay cases the kinetics of the decay is well described by the expression

$$N(t) = N_0 \exp\{-[t/\tau_0 + \gamma\sqrt{t} + \overline{W}t]\},$$ (30)

which confirms the result of the theory.[8] Our analysis shows that the function $\Pi(t)$ is, strictly speaking, of the form

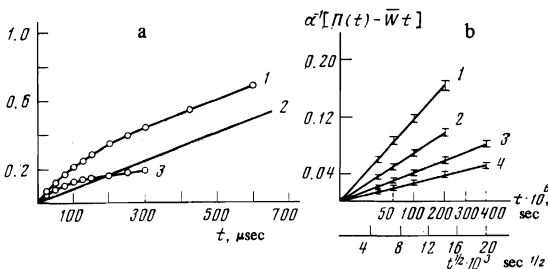$$W^{*}_{deact} = C_{DA}\Sigma(1/R^6) \qquad (31)$$

(the summation is over the sites of the lanthanum sublattice). The lattice sum in (31) was calculated on the basis of the data on the $LaF_3$ structure.[21] It turned out to be 0.008 Å$^{-6}$, whence

$$C_{DA}[sec^{-1} \cdot cm^6] = 1.22 \cdot 10^{-46} W^{*}_{deact}[sec^{-1}] . \qquad (32)$$

A plot of $C_{DA}(T)$ determined in this method is also shown in Fig. 10. We see that the values of $C_{DA}(T)$ determined by two independent methods are in good agreement. Some discrepancy at low temperatures is apparently due to the differences in the schemes of the crystal splitting at $C$ equal to 2 and 100 at.% $NdF_3$. Indeed, their analysis shows that at low temperatures the position of the lower component of the $^4I_{15/2}$ level is critical for the process of cross relaxation through this level, and its experimentally observed concentration shift can lead to concentration-dependent changes in the parameter $C_{DA}$, and also to differences in its temperature dependences at small and large $Nd^{3+}$ concentrations. When the temperature rises above 90 °K, a change of 20–30 cm$^{-1}$ in the energies of the interacting transitions is no longer significant, and the difference between the schemes of the crystal splitting does not influence the value of $C_{DA}$. Consequently, the parameter $C_{DA}$ turns out to be the same for all concentrations at temperatures higher than 90 °K.

Thus, the agreement between the values of $C_{DA}$ determined by independent methods indicates, on the one hand, that the nature of the direct annihilation of the electronic excitation remains the same at all concentrations, and serves, on the other, as a quantitative confirmation of the theory that connects the microscopic parameters of the interaction with the kinetics of the decay of the donor excitations under conditions of energy migration and direct donor-acceptor interactions, and, finally, confirms the result (30) and eliminates the leeway in the reduction of the experimental data when the asymptotic solutions of the theory (4) are used.

### Temperature dependence of $C_{DA}$

Let us analyze the temperature dependence obtained by us for $C_{DA}$. It is determined by the relative locations of the levels[2] $^4I_{9/2}$, $^4I_{15/2}$ and $^4F_{3/2}$. In the temperature region up to 45 °K, the activation energy in the temperature dependence of the $C_{DA}$ amounts to ~40 cm$^{-1}$, a fact naturally explained by the temperature population of the first excited Stark components of the ground and excited state $^4I_{9/2}$ and $^4F_{3/2}$. Indeed, at temperatures when the excited Stark components are not populated, the cross relaxation via the $^4I_{15/2}$ cannot be effected, since the energy difference between the ground Stark sublevels of the $^4F_{3/2}$ and $^4I_{15/2}$ multiplets is 38 cm$^{-1}$ smaller than the corresponding difference for the multiplets $^4I_{15/2}$ and $^4I_{9/2}$. Population of the first excited Stark components makes possible the transitions $^4F_{3/2} \to {}^4I_{15/2}$ and $^4I_{9/2} \to {}^4I_{15/2}$, the energies of which are respectively ~40 cm$^{-1}$ larger and ~40 cm$^{-1}$ smaller than the energies of the transitions between the corresponding ground-level Stark components, so that the cross relaxation via the $^4I_{15/2}$ level becomes possible. Exper-
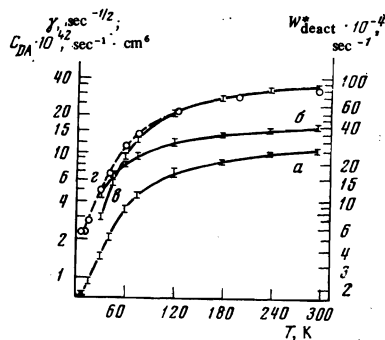


FIG. 10. Temperature dependences of the interaction parameters: a—$W^{*}_{deact}$, b—$\gamma$, c—of the parameter $C_{DA}$ determined on the basis of an analysis of the decay curves, d—of the parameter $C_{DA}$ determined on the basis of a calculation of the lattice sum.

$$\Pi(t) = \begin{cases} \gamma\sqrt{t}+\overline{W}t & \text{if} \quad t<t_2, \\ \overline{W}t+\Delta & \text{if} \quad t>t_2. \end{cases} \qquad (30a)$$

The meaning of the quantity $\Delta$ is clear from Fig. 8a. We can thus state that expression (29) is valid only at $t<t_2$. In the subsequent stages of the process, however, the second term in the exponent (30), just as $\Delta$, does not distort, within the limits of the measurement error, the exponential decay during the subsequent stages.

It must be emphasized that in all of the investigated cases the function $\Pi(t)$ retained, within the limits of the measurement errors, the same form at all $t$ down to $t=0$ (Fig. 8b). The apparent reason is the low concentration of the paired $Nd^{3+}$ centers in the $LaF_3$ lattice at small activator contents. On the other hand, when the concentration is increased, the time $t_2$ decreases and its non-exponential part, which is localized mainly in the time interval $t<t_2$, vanishes before the initial exponent of the decay can become noticeable ($t<t_1$). This occurs at $C>5$ at.% $NdF_3$. This is precisely the picture typical of the gradual transition to the simple migration mechanism of decay at $C_{DD} \gg C_{DA}$ (Fig. 7a), which comes into play at $t_2 \approx t_1$. We note that a short exponential section at times $t<t_1$ was observed by us in the crystal $YAlO_3-Nd^{3+}$, which has a large coordination number equal to 12, and in which, consequently, the number of pair clusters is large already at a content $Nd^{3+}$ 2 at.%.[9]

Knowing the temperature dependence of $\gamma(t)$ and using relation (19), we can determine the temperature dependence of $C_{DA}(T)$. Since the dependence of $\gamma$ on $C$ is linear (Fig. 9), it is natural for the values of $C_{DA}(T)$ to be the same for different concentrations. The result is shown in Fig. 10.

### The lattice-sum method

Figure 10 shows also a plot of $W_{deact}$ for the $NdF_3$ lattice ($W^{*}_{deact}$), which in the temperature region $>90$ °K duplicates exactly the course of the obtained temperature dependence of $C_{DA}$. As already noted, the values of the parameter $C_{DA}$ can be obtained by another independent method, using expression (11) and the measured value of $W^{*}_{deact}$.

iment has shown that it is precisely this relaxation which determines the temperature variation of $C_{DA}$. We shall call this nonradiative-relaxation channel the first channel.

At low temperatures, the cross relaxation via the $^4I_{15/2}$ level cannot be effected, but at concentrations $>2$ at.% $NdF_3$ nonradiative losses from the metastable state do take place also at $T = 4.2$ °K (Fig. 4). The reason for it is the existence of an additional decay channel via cross relaxation of the two intermediate levels $^4I_{13/2}$ and $^4I_{15/2}$ ($^4F_{3/2} \rightarrow {}^4I_{13/2} \cdot {}^4I_{9/2} \rightarrow {}^4I_{15/2}$) and the emission of phonons of appropriate energy.[14] Whereas the first channel can operate only at temperatures when the excited Stark components of the ground and excited states are populated, the second channel, which presupposes the delivery of phonons of considerable energy to the lattice, can lead to annihilation of the excitation at any temperature. It is natural to assume that the rate of decay in the second channel does not depend on the temperature (in the temperature range investigated by us), whereas relaxation via the first channel should be strongly temperature-dependent. We represent $C_{DA}$ in the form

$$C_{DA} = C_{DA}^{(I)} + C_{DA}^{(II)}, \qquad (33)$$

where $C_{DA}^{(I)}$ and $C_{DA}^{(II)}$ are the elementary parameters for the annihilation of the excitation in the first and second channels, respectively. On the basis of the foregoing, experiment makes it possible to determine $C_{DA}^{(I)}$ and $C_{DA}^{(II)}$ separately. Indeed, since $C_{DA}^{(I)}(T = 4.2-10 \text{ K}) \approx 0$, and $C_{DA}^{(II)}$ does not depend on $T$, it follows that $C_{DA}^{(II)} = C_{DA}(T = 4.2-10 \text{ K})$. The experimental value of $C_{DA}^{(II)}$ is $2.3 \times 10^{-42}$ sec$^{-1}$cm$^6$ (Fig. 10). An analysis of the curves in Fig. 10 shows that $C_{DA}^{(I)} \gg C_{DA}^{(II)}$ at $T > 120$ °K, i.e., at these temperatures only the first nonradiative-deactivation channel is operative.

When the temperature exceeds 45 °K, the activation energy in the temperature dependence begins to increase, a fact that may be due to phonon stimulation[22,23] and possibly to the large oscillator strengths of the transitions from the upper excited Stark components of the ground state of $^4I_{9/2}$ to the $^4I_{15/2}$ level and from the $^4F_{3/2}$ level to the excited Stark components of $^4I_{15/2}$. It must be noted that there are no exact resonances for the transitions $^4F_{3/2} \rightarrow {}^4I_{15/2}$ and $^4I_{9/2} \rightarrow {}^4I_{15/2}$, but there is a large number of combinations of transitions forming Stokes and anti-Stokes frequency differences with energies $\sim kT$. This gives rise to an appreciable contribution to the nonradiative deactivation
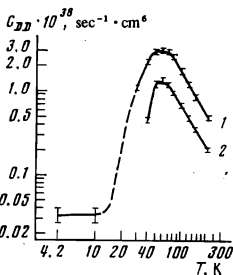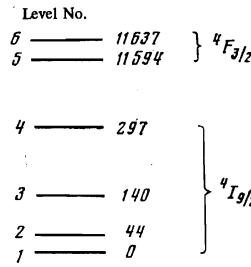


FIG. 12. Energy levels of the ground and excited states $^4I_{9/2}$ and $^4F_{3/2}$, respectively, which ensure energy migration in the investigated temperature region.

of processes with phonon participation and, as a consequence, to phonon stimulation.[22,23]

## Temperature dependence of $C_{DD}$

The aggregate of the results allows us also to determine the temperature dependence of $C_{DD}$. To this end it is necessary to use relations (6) and (9) as well as the obtained temperature dependences of $W(T)$ and $C_{DA}(T)$. The result is shown in Fig. 11. As seen from a comparison of Figs. 10 and 11, in the entire investigated temperature range the inequality $C_{DD} \gg C_{DA}$ is well satisfied, thus confirming the earlier conclusion that the energy dissipation due to migration to the acceptor is a random Markov process.

Let us attempt to describe the obtained temperature dependence within the framework of the resonant mechanism of energy migration. In the temperature range $4.2-300$ °K, energy migration may be the result of transitions between the levels shown in Fig. 12. The fifth Stark component of the ground multiplet is practically not populated in the temperature interval of interest to us. Then, if the spectrum has a Lorentz shape, the temperature dependence of $C_{DD}$ can be represented[19,20,24] in the form

$$C_{DD} = \text{const} \cdot \sum_i \sum_j \left( f_{i,j}^2 n_i n_j \frac{1}{\delta_{i,j}} \right), \qquad (34)$$

where $i = 1, 2, 3, 4$ are the numbers of the Stark components of the ground multiplet $^4I_{9/2}$, $j = 5$ and 6 are the numbers of the Stark components of the excited multiplet $^4F_{3/2}$, $f_{i,j}$ is the oscillator strength of the transition between the $i$-th and $j$-th components, $n_i$ and $n_j$ are the relative equilibrium populations of the $i$-th and $j$-th components of the corresponding multiplets, and $\delta_{i,j}$ is the homogeneous line width of the transition from the $i$-th to the $j$-th component.

An analysis of the luminescence and absorption spectra has shown that the narrowest intense lines are connected with the transitions $1 \rightarrow 6$, $1 \rightarrow 5$, and $2 \rightarrow 6$, i.e.,

$$C_{DD} \approx \text{const} \cdot \left[ f_{1,6}^2 n_1 n_6 \frac{1}{\delta_{1,6}} + f_{1,5}^2 n_1 n_5 \frac{1}{\delta_{1,5}} + f_{2,6}^2 n_2 n_6 \frac{1}{\delta_{2,6}} \right]. \qquad (35)$$

As seen from Fig. 12, the transitions $1 \rightarrow 5$ and $2 \rightarrow 6$ have the same energy. It turns out here that the quantity $\int k_{1,5}(\lambda)d\lambda$, where $k_{1,5}$ is the coefficient of absorption at the frequency of the $1 \rightarrow 5$ transition, does not depend on the temperature up to 100 °K. This indicates that $f_{1,5} = f_{2,6} = f$. It has also turned out that $f_{1,6} = 1.7f$. Putting $f = 1$, we obtain for $C_{DD}$



FIG. 11. Temperature dependence of $C_{DD}$: 1—experimental curve, 2—theoretical curve calculated from formula (36).

$$C_{DD} \approx \text{const} \cdot \left[1.7^2 n_1 n_6 \frac{1}{\delta_{1,6}} + \frac{1}{\delta}(n_1 n_5 + n_2 n_6)\right] \quad (\delta_{1,5} = \delta_{2,6} = \delta). \quad (36)$$

An analysis of the shapes of the spectral lines[25] has shown that the line of the $1 \to 6$ transition and the lines of the coinciding transitions $1 \to 5$ and $2 \to 6$ at $T > 50\,°K$ are homogeneously broadened. The temperature dependences of $\delta_{1,6}$ and $\delta$ were measured, and (36) was then used to plot the temperature dependence of $C_{DD}$. This plot is shown in Fig. 11. It is seen that the calculated temperature dependence has the same form as the experimental one. At high temperatures their slopes coincide exactly, and at low temperatures the experimental plot differs somewhat from the calculated one. The apparent reason is that at low temperatures inhomogeneous broadening, which becomes predominant at $T = 4.2\,°K$, begins to contribute to the line width of the $1 \to 5$ transition.

As shown in[19,20], the decrease of the homogeneous width of the spectral line compared with the inhomogeneous one is accompanied by the appearance of a temperature dependence of the resonant migration in the corresponding temperature range. From the point of view developed in[20] it is easy to explain also the presence of the plateau on the $C_{DD}(T)$ curve at low temperatures. It can be due to the temperature mismatch of the Lorentz contours of the lines, which is caused by the ions situated in neighboring coordination spheres.[20] It should be noted that we do not know the exact temperature dependence of $C_{DD}(T)$ in the narrow temperature region $10-30\,°K$ (Fig. 11), since the values of $C_{DA}(T)$ determined at low and high concentrations differ somewhat at low temperatures, and we do not know the values of $C_{DA}(T)$ at low concentrations in the indicated temperature region (Fig. 10).

The foregoing analysis of the temperature dependence of $C_{DD}$ has shown that the phonon-stimulation effect does not manifest itself in the energy migration over the $Nd^{3+}$ ions, that the migration is resonant, and that its effectiveness is determined by the populations of the corresponding Stark components, by the oscillator strengths, by the homogeneous broadening, and by the ratio of the homogeneous and inhomogeneous components of the interacting transitions.

Thus, the obtained temperature dependences of the microscopic parameters of the interaction explain all the experimentally obtained regularities, and in particular the absence of nonradiative losses in the temperature range $4.2-10\,°K$ at $C = 2$ at.% $NdF_3$ and their presence at $C > 2$ at.% $NdF_3$. Indeed, substituting the obtained values of the parameters $C_{DA}$ and $C_{DD}$ in (6) or (9), we find that at $C = 2$ at.% $NdF_3$ we have $\bar{W} = 80\,\text{sec}^{-1}$ at a total radiative probability $1/\tau_0 = 1340\,\text{sec}^{-1}$, i.e., the condition $1/\tau_0 \gg \bar{W}$ is satisfied and no nonradiative losses from the metastable state are observed. On the other hand, when the concentration is increased to 3 at.% $NdF_3$, $\bar{W}$ becomes equal to $180\,\text{sec}^{-1}$ and a certain decrease of $\tau_{\text{meas}}$ becomes already noticeable.

Let us summarize our main results.

We obtained experimentally the form of the kinetics of the decay of donor excitations under conditions of energy migrations and direct donor-acceptor interactions. We separated the sections of the static-ordered, static-disordered, migration, and supermigration decays. We have shown that at large activator concentrations the decay of the metastable state takes place under conditions of energy supermigration. Expressions were obtained for the critical concentrations and the times of transitions of one type of decay into another. Two independent methods were used to determine the microscopic interaction parameter $C_{DA}$ and its temperature dependence. We have shown that the energy migration over the neodymium ions is not of the diffusion type, and the annihilation of the electronic excitation due to the migration of the excitations to the energy acceptors is a random Markov process. We determined the contributions made to the nonradiative decay by cross relaxation via one intermediate level $^4I_{15/2}$ and via two intermediate levels $^4I_{13/2}$ and $^4I_{15/2}$. We have shown that energy migration over a metastable state of neodymium is due to resonant dipole–dipole interaction.

---

[1])The term "ultrafast energy migration" was proposed in[7]. For the sake of brevity we shall call this "supermigration." Its meaning will be explained later on. It must be emphasized only that the interaction that leads to supermigration remains incoherent in the sense that the rate of phase relaxation is still a faster process and consequently the probabilistic approach is still valid.

[2])The level scheme of the $Nd^{3+}$ ion in the $LaF_3$ crystal is given in[14].

[1]B. C. Tofield, H. P. Weber, T. C. Damen, and P. F. Liao, J. Solid State Chem. 12, 207 (1975).
[2]I. A. Bondar', T. G. Mamedov, L. P. Mezentseva, I. A. Shcherbakov, and A. I. Domanskii, Kvantovaya Elektron. (Moscow) 1, 2625 (1974) [Sov. J. Quantum Electron. 4, 1463 (1975)].
[3]C. K. Asawa and M. Robinson, Phys. Rev. 141, 251 (1966).
[4]I. V. Vasil'ev, G. M. Zverev, G. Ya. Kolodnyi, and A. M. Onishchenko, Zh. Eksp. Teor. Fiz. 56, 122 (1969) [Sov. Phys. JETP 29, 69 (1969)].
[5]M. Yokota and O. Tanimoto, J. Phys. Soc. Jap. 22, 777 (1967).
[6]M. V. Artamonova, Ch. M. Briskina, A. I. Burshtein, L. D. Zusman, and L. G. Skleznev, Zh. Eksp. Teor. Fiz. 62, 863 (1972) [Sov. Phys. JETP 35, 457 (1972)].
[7]A. I. Burshtein, ibid., 1695 [882].
[8]V. P. Sakun, Fiz. Tverd. Tela (Leningrad) 14, 2199 (1972) [Sov. Phys. Solid State 14, 1906 (1973)].
[9]Yu. K. Voron'ko, T. G. Mamedov, V. V. Osiko, M. I. Timoshechkin, and I. A. Shcherbakov, Zh. Eksp. Teor. Fiz. 65, 1141 (1973) [Sov. Phys. JETP 38, 565 (1974)].
[10]V. M. Agranovich, Teoriya eksitonov (Exciton Theory), Nauka, 1968.
[11]T. T. Basiev, T. G. Mamedov, and I. A. Shcherbakov, Kvantovaya Elektron. (Moscow) 2, 1269 (1975) [Sov. J. Quantum Electron. 5, 687 (1975)].
[12]T. T. Basiev, Yu. K. Voron'ko, T. G. Mamedov, V. V. Osiko, and I. A. Shcherbakov, in: Spektroskopiya kristallov (Spectroscopy of Crystals), Nauka, 1975, p. 155.
[13]A. A. Kaminskii and V. V. Osiko, Izv. Akad. Nauk SSSR Neorg. Mater. 1, 2049 (1965); 3, 417 (1967).
[14]Yu. K. Voron'ko, V. V. Osiko, N. V. Savost'yanova, V. S. Federov, and I. A. Shcherbakov, Fiz. Tverd. Tela (Leningrad) 14, 2656 (1972) [Sov. Phys. Solid State 14, 2294 (1973)].
[15]T. T. Basiev, Prib. Tekh. Eksp. No. 2, 182 (1976).
[16]T. T. Basiev, E. M. Dianov, A. M. Prokhorov, and I. A. Shcherbakov, Dokl. Akad. Nauk SSSR 216, 297 (1974) [Sov.

260     Sov. Phys. JETP, Vol. 44, No. 2, August 1976

Voron'ko et al.     260

Phys. Dokl. 19, 288 (1974)].
[17]E. M. Dianov, A. Ya. Karasik, V. B. Neustruev, A. M. Prokhorov, and I. A. Shcherbakov, Dokl. Akad. Nauk SSSR 224, 64 (1975) [Sov. Phys. Dokl. 20, 622 (1975)].
[18]A. I. Burshteĭn and A. Yu. Pusek, Fiz. Tverd. Tela (Leningrad) 16, 2318 (1974) [Sov. Phys. Solid State 16, 1509 (1975)].
[19]T. T. Basiev, Yu. K. Voron'ko, and I. A. Shcherbakov, Zh. Eksp. Teor. Fiz. 66, 2118 (1974) [Sov. Phys. JETP 39, 1042 (1974)].
[20]T. T. Basiev, Yu. K. Voron'ko, T. G. Mamedov, and I. A. Shcherbakov, Kvantovaya Elektron. (Moscow) 2, 2172 (1975) [Sov. J. Quantum Electron. 5, 1182 (1975)].

[21]B. F. Ormont, Struktura neorganicheskikh veshchestv (Structure of Inorganic Substances), Gostekhizdat, 1950.
[22]T. Miyakawa and D. L. Dexter, Phys. Rev. B1, 2961 (1970).
[23]Yu. K. Voron'ko, V. V. Osiko, and I. A. Shcherbakov, Zh. Eksp. Teor. Fiz. 63, 691 (1972) [Sov. Phys. JETP 36, 365 (1973)].
[24]D. L. Dexter, J. Chem. Phys. 21, 836 (1953); A. S. Agabekyan, Proc. 3rd All-Union Seminar on Nonradiative Energy Transfer in Condensed Media, Erevan, 1950, p. 53.
[25]D. W. Posener, Aust. J. Phys. 12, 184 (1959).

Translated by J. G. Adashko

# Scattering of electrons by inert gas atoms with ejection of one or two electrons from the outer shell

S. G. Shchemelinin, E. P. Andreev, N. A. Cherepkov, and S. I. Sheftel'

A. F. Ioffe Physico-technical Institute, USSR Academy of Sciences
(Submitted March 4, 1976)
Zh. Eksp. Teor. Fiz. 71, 497–510 (August 1976)

Beam electrons inelastically scattered by He, Ne or Ar atoms are separated by a coincidence technique into components due to single or double ionization of the outer shells. The initial electron energy is 4 keV and the scattering angle range is 0–10°. The energies transferred do not exceed the ionization threshold for the inner shells. The absolute values of the differential cross sections for single and double ionization are measured as functions of two variables, the transferred energy and the scattering angle. The generalized oscillator strengths (GOS) for single and double ionization are determined from the measured momentum transfers up to 3 atomic units. At small values of the transferred momenta the GOS are consistent with available optical data for both single and double ionization. The dependences of the double-ionization GOS on the transferred momentum has a characteristic peak whose position is practically identical with that of the single-ionization GOS. On the other hand a difference in the shapes of the curves of the single and double ionization GOS as a function of momentum transfer is observed. The magnitude and character of the difference depend on the atom. The narrower GOS peak is related to double ionization via the virtual Auger effect. The argon single-ionization GOS are calculated in the RPAE approximation. It is shown that the calculation, in effect, also takes into account multiple ionization.

PACS numbers: 34.70.Di

## 1. INTRODUCTION

One of the methods of investigating the structures of atoms and molecules is to study the angular and energy distributions of the electrons scattered by them. [1,2] At sufficiently high electron energies, these experiments yield the generalized oscillator strengths (GOS), which are connected in the Born approximation with the differential inelastic-scattering cross sections. [3] The GOS depend on two parameters, the energy and momentum given up in the collision, and the set of these parameters constitutes a two-dimensional spectrum that provides a more complete description of the target [4,5] than the optical photoabsorption spectrum; the latter is the limiting case of the GOS at zero momentum transfer. The GOS measured in this manner turn out to be summed over the final states of the target.

The influence of the electron–electron interactions in the atom (correlations) on the elastic scattering of fast electrons was explained in earlier papers. [1,4,5] In the present paper we study the inelastic-scattering components that are connected with a definite multiplicity of the target ionization and have been separated by the coincidence method.

Multiple ionization, as all many-electron transitions in general, is due to the interaction of the target electrons with one another. Even to explain the existence of such transitions it is necessary to take the interelectron interactions into account in greater detail than in the Hartree–Fock method (assuming the self-consistent field to be the same). [6] The oscillator strengths of many-electron transitions have been investigated up to now, both theoretically and experimentally, only in the optical limit.

Attempts at a quantitative description of two-electron transitions are being undertaken in two directions—by taking into account the interelectron correlations in the wave functions, as well as with the aid of many-body quantum theory. The first of these methods is limited to light atoms (results are available for He [7,8]) and its success depends on the proper choice of the form of the wave functions. The second method [9] is more consistent and is suitable for both light [16] and heavy [9,11]